Journal of ELECTRONIC MATERIALS, Vol. 41, No. 10, 2012
DOI: 10.1007/s11664-012-2007-8

Investigation of Structural Defects in CdZnTe Detector-Grade Crystals

A. HOSSAIN,[1,2] A.E. BOLOTNIKOV,[1] G.S. CAMARDA,[1] R. GUL,[1] K.H. KIM,[1] K. KISSLINGER,[1] G. YANG,[1] L.H. ZHANG,[1] and R.B. JAMES[1]

1.—Brookhaven National Laboratory, Upton, NY 11973, USA. 2.—e-mail: hossain@bnl.gov

We investigated structural defects in CdZnTe detector-grade crystals grown under different conditions. Here, we report our findings from high-resolution electron microscopy [transmission electron microscopy (TEM) and scanning TEM (STEM)] and scanning electron microscopy integrated with energy-dispersive x-ray spectroscopy to characterize the material's structural and chemical composition. Combining these techniques gave us important information about the defects, their concentration, and the elemental composition of the CdZnTe crystals. Our experimental observations demonstrated some distinct nanostructural defects in the crystals that may play a major role in device performance.

Key words: CdZnTe, radiation detectors, TEM, stacking faults, dislocations, Te precipitate

INTRODUCTION

At present, CdZnTe undoubtedly is the leading material for room-temperature radiation detectors. However, its widespread deployment is limited by the high-cost materials due to limited defect-free large-volume yields. CdZnTe still suffers from various point and extended defects, such as inclusions, dislocations, low-angle grain boundaries, and precipitates, primarily generated during crystal growth and the postgrowth cooling process.[1,2] Some of these defects are well defined; however, structural and chemical compositional defects, e.g., stacking faults, dislocations, and impurities, are not readily identifiable using conventional techniques because they are very small, ranging down to the nanoscale level; nevertheless, they inevitably degrade overall device performance.[3,4] We investigated such crystalline defects in CdZnTe using transmission electron microscopy (TEM) and scanning electron microscopy (SEM) integrated with energy-dispersive x-ray spectroscopy (EDS) and transmitted electron detection (TED). These techniques allowed us to observe directly such structural defects and other related ones, and to acquire information on the chemical composition of CdZnTe crystals. We specified our findings in terms of the defects' concentration, size, and phase. Our experimental observations demonstrated distinct nanostructural defects in the crystals, such as dislocations and precipitates. Reportedly, these defects are the major causes of degradation of the electrical properties of the devices, ultimately limiting their performance as x-ray and gamma-ray spectrometers.[5–7]

(Received November 7, 2011; accepted February 10, 2012; published online March 9, 2012)

EXPERIMENTAL PROCEDURES

In this work, samples were selected from detector-grade $Cd_{0.9}Zn_{0.1}Te$ crystals grown by high-pressure Bridgman method.[8,9] The resistivity and mobility–lifetime values of the samples were in the range of $10^{10}\ \Omega\,cm$ to $10^{11}\ \Omega\,cm$ and $\sim 7 \times 10^{-3}\ cm^2/V$, respectively. TEM samples were prepared by the lift-off method inside a Helios dual-beam SEM/FIB system and then exposed to a focused ion beam (FIB) to thin them to around 100 nm to become electron transparent. The samples were mounted on and glued to their copper holders with Pt gas. Pt/Au was deposited on top of the samples to prevent charging, as the material's resistivity is very high. We studied six CdZnTe samples via TEM

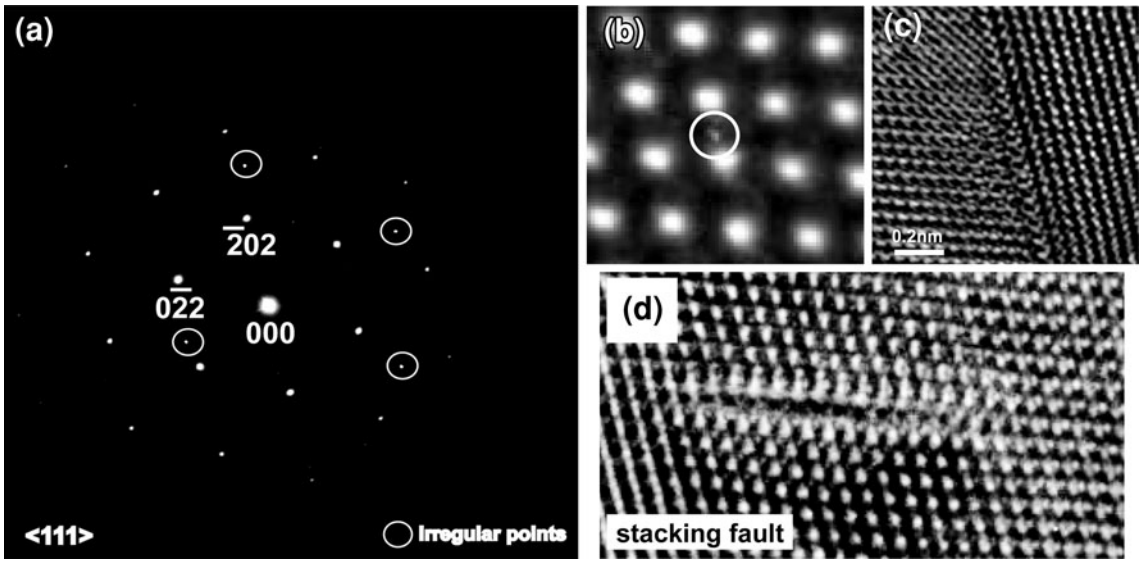

Fig. 1. (a) SAD pattern of CdZnTe crystal at the ⟨111⟩ plane, wherein some irregular points in white circles indicate the existence of imperfections of the crystal lattice; (b) interstitial atom traced in the lattice plane; (c) low-angle grain boundary: distortion in the lattice structure extended beyond the defect region; (d) a typical stacking fault in the CdZnTe matrix.

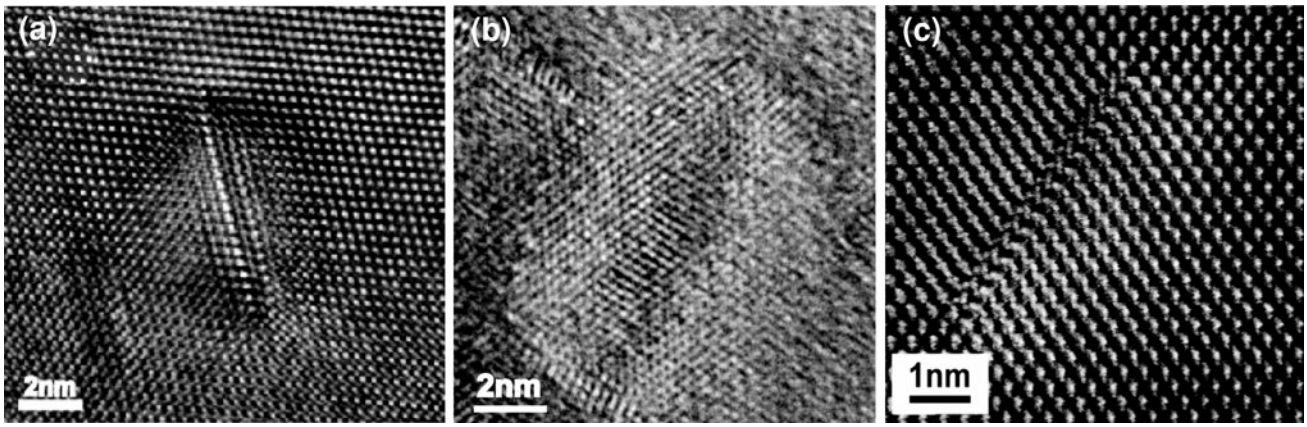

Fig. 2. (a) Stacking fault turning into dislocation loop; (b) dislocation loop; (c) stacking fault disappearing, leaving behind a misfit dislocation.

(JEOL-2100F, Hitachi HD2700C) and SEM–EDS (JEOL7600F).

RESULTS AND DISCUSSION

Figure 1a displays a representative image of a selected-area diffraction (SAD) pattern on a CdZnTe ⟨111⟩ projection taken from a random area. The irregular points in the diffraction pattern encircled in white indicate the presence of some kinds of defects in this area; they could be twins, dislocations, or impurities. Using a high-resolution electron microscope, we recorded images of the CdZnTe matrix at those selected areas, and traced various defects distributed randomly, such as the two shown in Fig. 1b, c. At this stage of our research, we have not fully characterized those entities, nor recorded their impact on device performance.

We also observed various other defects in the crystalline structure distributed irregularly within its matrix. Among them, stacking faults were one of the most common extended defects traced in the specimens. Figure 1d shows a typical stacking fault found in the matrix. It is a long-range interruption in the stacking sequence of molecules, and the difference in the potential energy of the inner and outer layer of the stacking molecules determines the fault's width and may eventually diminish, leaving behind plastic deformation in the matrix, often represented in the form of a dislocation loop or a misfit dislocation.[10] Figure 2 illustrates the transformation of a stacking fault into a dislocation loop and other type of dislocation. The concentration of such defects was roughly estimated to be in the range of 10^2 μm^{-2} to 10^3 μm^{-2}, and they are present nonuniformly throughout the matrix. We also noticed that the quantity of these defects is much higher in our samples compared with that of other defects, such as impurities and vacancies.

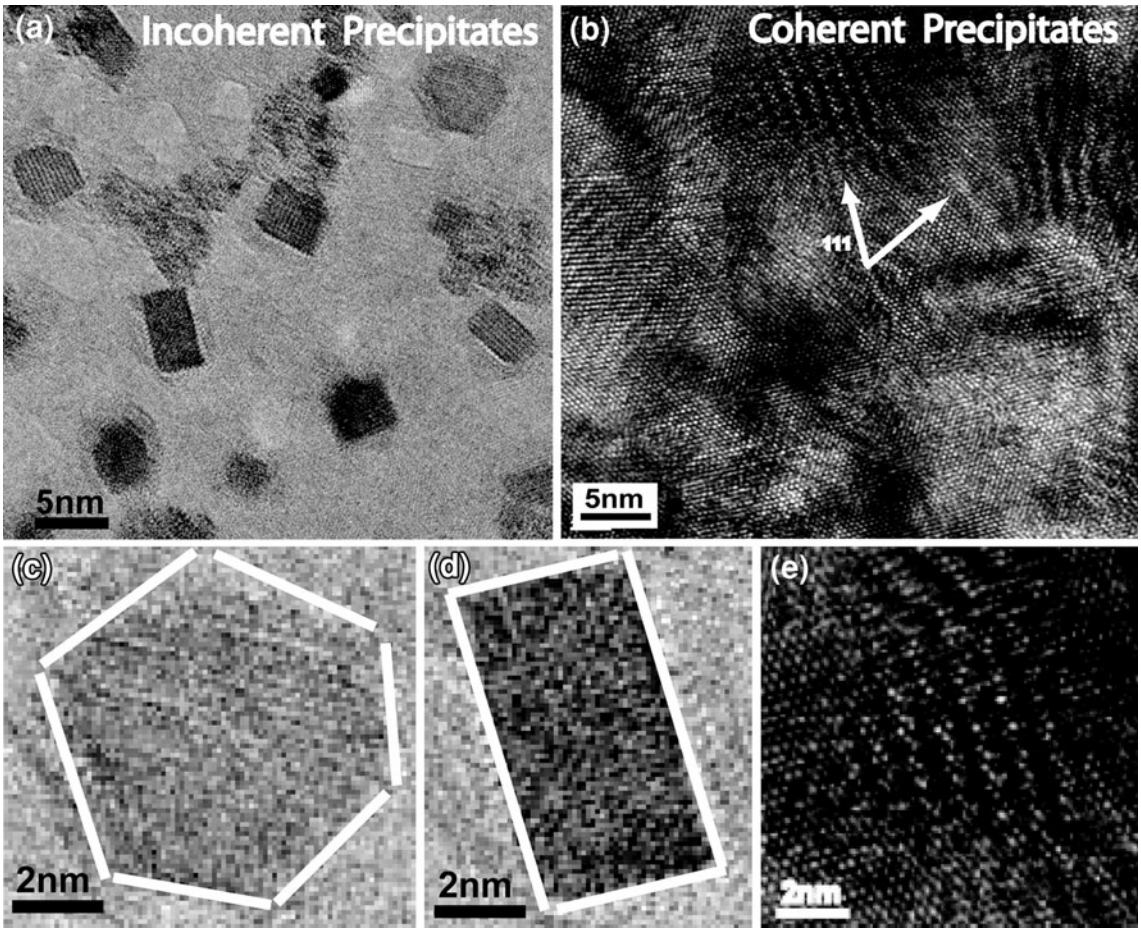

Fig. 3. TEM micrographs of a CdZnTe matrix: (a) Te precipitates arranged incoherently in the matrix with some definite shape; (b) Te precipitates blended in the matrix; (c–e) magnified images of Te precipitates lying coherently and incoherently in the lattice.

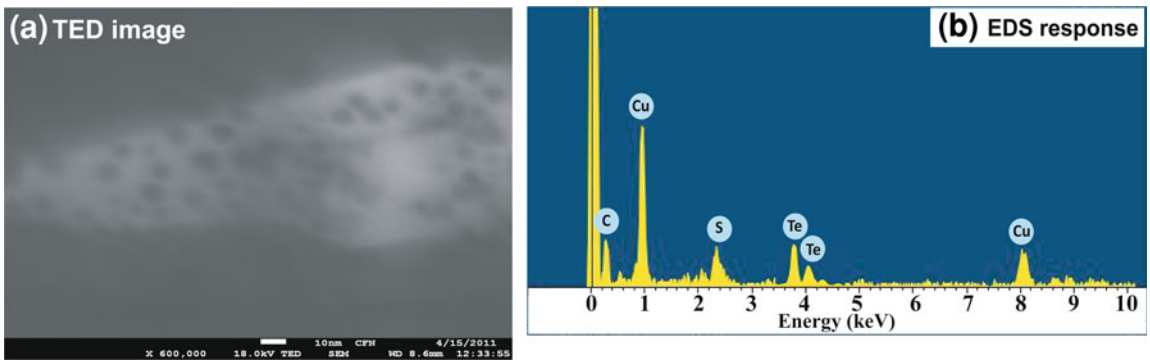

Fig. 4. (a) Image captured by TED using a SEM JEOL7600F system; (b) EDS spectral response of CdZnTe TEM specimen shown in (a). The dark spots in the TED image were identified as Te precipitates. Cu signal is definitely coming from the sample holder, but the origin of the sulfur (S) peak was not confirmed.

Figure 3a–e shows many small, dark, irregularly shaped objects that are nonuniformly distributed in the CdZnTe matrix, either coherently (matched with matrix) or incoherently (random with matrix). These spots range from 5 nm to 20 nm, and their concentration was as high as 10^{12} cm^{-2}. Wang et al.[11] regarded them as Te precipitates, and described them in detail. Rudolph[12] considered that they generally originate from the solubility of retrograde solids during the postgrowth cooling process. However, their influence on device performance is hardly documented, because they are too small to be identified by conventional techniques.

In this work, we employed SEM integrated with EDS, and TED to confirm those black spots shown in Fig. 3 and also mentioned in Ref. 9. Figure 4

displays captured images of those black spots, and the extracted EDS signal from a focused electron beam on one of the spots. The EDS spectra convinced us that those small objects mainly are Te precipitates. More experiments are underway to ascertain whether these precipitates are in elemental or complex form.

CONCLUSIONS

Our experimental observations demonstrated distinct structural defects in the crystals, such as stacking faults, dislocation loops, and Te precipitates. Stacking faults and dislocation loops generate plastic deformation in the crystal lattice that extends beyond the defect region. Also, we found multiple small Te precipitates existing randomly in the crystal matrix. Further analyses are needed to fully identify their nature and detail their effects on device performance.

REFERENCES

1. C. Szeles, S.E. Cameron, J.-O. Ndap, and W.C. Chalmers, *IEEE Trans. Nucl. Sci.* NS-49, 2535 (2002).
2. A.E. Bolotnikov, S.O. Babalola, G.S. Camarda, H. Chen, S. Awadalla, Y. Cui, S.U. Egarievwe, P.M. Fochuk, R. Hawrami, A. Hossain, J.R. James, I.J. Nakonechnyj, J. Mackenzie, G. Yang, C. Xu, and R.B. James, *IEEE Trans. Nucl. Sci.* NS-56, 1775 (2009).
3. J.R. Heffelfinger, D.L. Medlin, and R.B. James, *Semiconductors for Room Temperature Radiation Detector Applications II*, Vol. 487, ed. R.B. James, T.E. Schlesinger, P. Siffert, W. Dusi, M.R. Squillante, M. O'Connell, and M. Cuzin (Pittsburgh, PA: Materials Research Society, 1988), p. 33.
4. T.E. Schlesinger, J.E. Toney, H. Yoon, E.Y. Lee, B.A. Brunett, L. Franks, and R.B. James, *Mater. Sci. Eng.* R32, 103 (2001).
5. G.A. Carini, A.E. Bolotnikov, G.S. Camarda, G.W. Wright, L. Li, and R.B. James, *Appl. Phys. Lett.* 88, 143515 (2006).
6. A.E. Bolotnikov, S.O. Babalola, G.S. Camarda, Y. Cui, R. Gul, S.U. Egarievwe, P.M. Fochuk, M. Fuerstnau, J. Horace, A. Hossain, F. Jones, K.H. Kim, O.V. Kopach, B. McCall, L. Marchini, B. Raghothamchar, R. Taggart, G. Yang, L. Xu, and J.R. James, *IEEE Trans. Nucl. Sci.* NS-58, 1972 (2011).
7. A. Hossain, A.E. Bolotnikov, G. Camarda, Y. Cui, G. Yang, K.-H. Kim, R. Gul, L. Xu, and R.B. James, *J. Cryst. Growth* 312, 1795 (2010).
8. K.B. Parnham, *Nucl. Instrum. Methods Phys. Res.* A377, 487 (1996).
9. F.P. Doty, J.F. Butler, J.F. Schetzina, and K.A. Bowers, *J. Vac. Sci. Technol.* B10, 1418 (1992).
10. A. Kuronen, K. Kaski, and L.F. Perondi, *Europhys. Lett.* 55, 19 (2001).
11. T. Wang, W. Jie, and D. Zeng, *Mater. Sci. Eng. A* 472, 227 (2008).
12. P. Rudolph, *Cryst. Res. Technol.* 38, 542 (2003).